International Journal on Recent and Innovation Trends in Computing and Communication
ISSN: 2321-8169 Volume: 11 Issue: 9
Article Received: *25 July 2023* ***Revised:*** *12 September 2023* ***Accepted:*** *30 September 2023*

Design and Performance Analysis of a Neural Network Sliding Mode based Hybrid Controlled Islanded Micro-Grid

A. Venkat Rao [1], Dr. G. Suresh Babu [2], Dr. P. Satish Kumar [3]

[1] Research scholar, Department of Electrical Engineering, Osmania University, Hyderabad, Telangana, India.
Email: venki.aarepalli@gmail.com
[2] Professor, Department of Electrical and Electronics Engineering, Chaitanya Bharathi Institute of Technology, Telangana, India.
Email: gsureshbabu_eee@cbit.ac.in
[3] Professor, Department of Electrical Engineering, Osmania University, Hyderabad, Telangana, India.
Email: satish_8020@yahoo.co.in

Abstract:

The micro-grid fed shunt voltage source converter, also known as a smart Artificial neural network and sliding mode controller (ANN-SMC) based hybrid system, is developed during this research for solar system, wind and battery storage connected shunt filter. Here, phased locked loop utilization is avoided by the self-tuning filter (STF). Move over, apart from producing phase synchronization, STF also distinguishes between the fundamental and harmonic components. Total harmonic distortion (THD) reduction and steady voltage across dc link during load variations with short settling times under both grid and island settings are the key goals of the recommended approach. Four scenarios with various combinations of loads, solar radiation, and wind speeds under islanding conditions are used to illustrate the effectiveness of the study.

Index Terms: Self tune shunt active power filter, Total harmonic distortion, solar PV system, Wind system, Battery energy storage.

1. INTRODUCTION

PQ issues arise in the network of distribution as a result of the use of power electronic devices in conjunction with renewable energy sources. The power engineers are faced with a problem in managing these issues' negative repercussions. In addition to the latest developments, the different SAPF control strategies and setups for distribution networks were examined [1]. Besides, for the four-phase system of distribution with balanced and unbalanced loads, the synchronous reference frame theory (SRFT) control system was recommended [2]. In order to reduce the THD for various types of loads, fuzzy logic controller (FL-C) and propotional integral controller (PI-C) attributes were merged to create a hybrid controller for shunt active power filter(STAPF) [3]. In addition, the STF-based STAPF was created to control the present signal THD in addition to reactive and actual powers [4]. Additionally, improvements in artificial intelligence control techniques, such as FL-C, ANNC, and others, for STAPF effectively handle PQ problems during fluctuations in the constantly changing load on the system [5-7].

The adopted model, named the Grey Wolf Insisted Inertia-based Path finding Algorithm, is employed for this optimal choice. The proposed model takes into account factors such as voltage index stability, power loss, and UPQC budget to determine the optimal installation location for a UPQC device [8]. An Adaptive Neuro-Fuzzy controller incorporates a reinforcement learning algorithm to examine the configured system. Employing language-based concepts for inferring system parameters, the Fuzzy Model-Based (FMB) controllers enhance system efficiency and contribute to generating current references [9]. In the event of changing system parameters, a versatile Fuzzy Logic Controller (FLC) is deployed. The Unified Power Quality Conditioner (UPQC) is subjected to both static and switching nonlinear loads. This configuration enables the UPQC to eliminate harmonics, reduce voltage fluctuations, and mitigate sag/swell issues [10]. This study introduces an adaptive controller inspired by Genetic

International Journal on Recent and Innovation Trends in Computing and Communication
ISSN: 2321-8169 Volume: 11 Issue: 9
***Article Received:** 25 July 2023 **Revised:** 12 September 2023 **Accepted:** 30 September 2023*

Algorithms for compensating PQ issues and regulating the DC-link voltage in the UPQC system. The proposed approach effectively generates an optimal DC-link voltage regulation [11].

In the presented microgrid design, careful consideration is given to incorporating a robust UPQC, commonly employed alongside conventional sources, to manage voltage and power flow. The UPQC in MATLAB software has undergone additional optimization through the implementation of the ANFIS approach [12]. This study introduces an ANN-based control system for a UPQC employing the LMBP algorithm. The proposed power distribution system encompasses a five-level diode clamped converter. Various challenging troubles like, including L-G, L-L-G, and L-L-LG faults, are considered for analysis. Within this framework, an ANN based PAA control is developed to transfer reactive power between parallel and series converters without increasing the VSC rating, thereby reducing the overall system cost [13]. This research introduces a comprehensive active power filter designed for microgrid systems incorporating renewable energy sources. In this approach, the DC-link of the APF integrates the battery storage system with renewable sources such as solar and wind. The proposed microgrid system employs a Centralized Microgrid Controller to enhance PQ and effectively control power flow. The primary objectives of the CMC include optimizing the utilization of Renewable Energy Sources , ensuring smooth power transfer across various operational scenarios, and providing a reliable and high-quality power supply to the connected load [14]. To precisely mitigate current and harmonic distortions in UPQC-connected medical equipment, it is suggested to employ a novel PI-C based on the Adaptively Updating Sparrow Search Algorithm. This controller has been seamlessly integrated with sustainable energy sources like Squirrel Cage Induction Generators from wind turbines [15]. To obviate the need for LPFs and PLL to reduce the THD, the STAPF with STF was created. Conversely, the outcomes are confirmed using an experimental configuration [16].

The proposed model incorporates four distinct compensating elements—UPFC, DPFC, USSC, and UPQC—to improve the power quality of the system. Utilizing a benchmark dataset in real-time, encompassing various power quality conditions such as harmonics, sag, swell, and interruptions, a deep learning intelligent controller model is developed. This model is based on the collected dataset and governs the system, ensuring a continuous and stable power supply [17]. However, the implementation of UPQC algorithms and control techniques to improve PQ implies the need for a versatile control strategy aimed at enhancing UPQC efficiency. The proposed dynamic regulation technique demonstrates enhanced steady-state and dynamic performance, as evidenced by testing on a critical distribution network [18]. Besides, a unit vector template control approach is employed to utilize the single-phase Unified Power Quality Conditioner (UPQC) for grid-integrated photovoltaic operations. This includes tasks such as addressing voltage sags/swells, correcting unit power factor, and cancelling voltage and current harmonics. The unit vector template control algorithm incorporates a phase-locked loop (PLL) technique to prevent multiple zero crossings during the detection of severely distorted grid voltage. For the UPQC dependent on the PV grid, the unit vector template control with a PLL-based control algorithm is applied to both the shunt and series inverters [19].

This work suggests using ANN-SMC for the micro-grid connected to STAPF in order to reduce THD as an objective function under islanding conditions and stabilise DLCV during load changes with the shortest settling time. In order to prevent the need for PLL, the STAF is suggested. In order to illustrate the efficiency of ANN-SMC, four distinct test studies are conducted. The article is organized as follows: Section 2 describes the suggested system, Section 3 offers the control technique, Section 4 presents the findings and the discussion, and the sixth section concludes with a summary of the results.

2. DEVELOPED SYSTEM

Fig. 1 shows the constructed STAPF with all of its elements. The microgrid and STAPF are connected via a DC Link, which uses boost converter (B-C) for photovoltaic panels and buck-boost converter (B-B-C) for batteries. Shunt-linked VSCs are primarily responsible for reducing current THD by providing the necessary compensated current for DC link balancing.

Table 1: PV, Wind and BES ratings

Equipment	Factor	Value chosen
	PV cells connected in parallel, series	66, 5

International Journal on Recent and Innovation Trends in Computing and Communication
ISSN: 2321-8169 Volume: 11 Issue: 9
Article Received: *25 July 2023* ***Revised:*** *12 September 2023* ***Accepted:*** *30 September 2023*

PV single panel (Sun power SPR-305E-WHT-D)	Rated Power	305.226W
	Short circuit current	5.98A
	Open circuit voltage	64.2V
	Under max power the voltage & current	54.7V /5.58A
	Fully charge voltage	350V
Li-ion battery	Rated Capacity of battery	350Ah
	Cut off voltage	262.5V
	Normal Voltage	405V
Wind Turbine	Nominal turbine mechanical power	4 MW
	Base power of the electrical generator	400e3/0.9
	Base wind speed	11 m/sec

The STAPF receives an outside feed from the microgrid that consists of solar, wind, and battery energy systems to control the DC capacitor balance under varying loading circumstances. The primary benefit of external renewable source support, however, is a decrease in the converters' burden and necessary ratings. The micro grid values selected for this work are listed in Table 1. Table 2 provides a description of the power distribution for the proposed STAPF at the capacitor, which is displayed by Equation (1).

$$P_{PV} + P_{BS} - P_{DC} = 0 \quad (1)$$

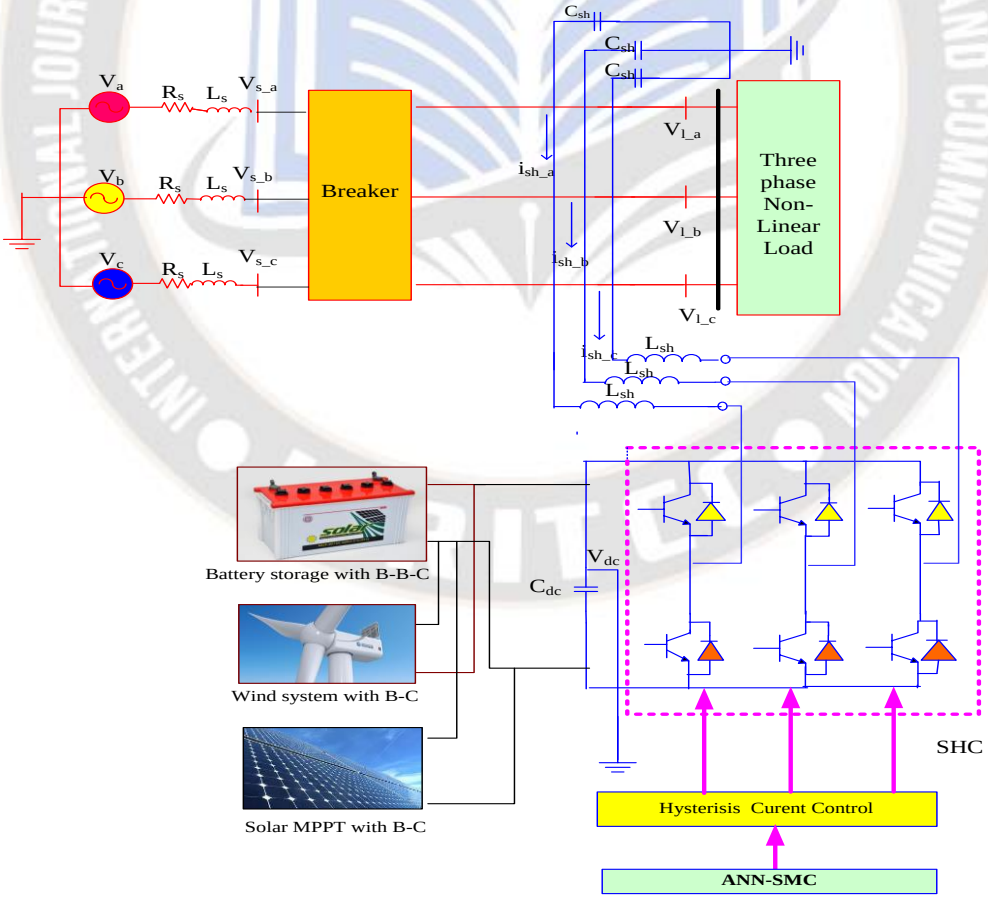

Figure 1: Components of STAPF

International Journal on Recent and Innovation Trends in Computing and Communication
ISSN: 2321-8169 Volume: 11 Issue: 9
Article Received: *25 July 2023* ***Revised:*** *12 September 2023* ***Accepted:*** *30 September 2023*

2.1 Solar PV system

The PV (photovoltaic) modules combined in parallel or series influence how much radiation from the sun is converted into energy by the solar PV system. Each PV cell in the module is modelled using a circuit equivalent of a single diode, as shown in Fig 2.

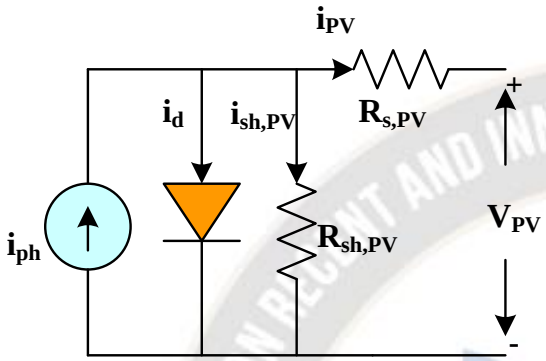

Figure 2: PV cell model

The components of it are a resistances ($R_{s,PV}$ and $R_{sh,PV}$) carrying the current of (i_{PV}, $i_{sh,PV}$), a photocurrent (i_{ph}) with a forward diode current (i_d). Solar energy is detected by the PV cell, which then transforms it into current. PV current (i_{PV}) can be achieved by applying KCL, as shown by Eq. (2)

$$i_{PV} = i_{ph} - i_d - i_{sh,PV} \quad (2)$$

Where,

$$i_d = i_{rev,sat}(e^{\frac{V_d}{\eta V_T}} - 1)$$

$$i_{rev,sat} = K(T^m)(e^{\frac{-V_{G0}}{\eta V_T}}) and \quad (3)$$

$$V_T = \frac{K_B}{q}T$$

Here, $i_{rev,sat}$ is the reversal saturated current; V_{G0} indicates the band width of the material taken into consideration in ev; T represents the temperature; K_B is the Boltzmann constant and η is the diode identification factors. We may obtain the cell's current by using Eq. (4) by inserting Eq. (3) into Eq. (2).

$$i_{PV} = i_{ph} - i_{rev,sat}(e^{\frac{V_d}{\eta V_T}} - 1) - \frac{V_{PV} + I_{PV}R_{sh,PV}}{R_{sh}} \quad (4)$$

In this work, the MPPT method based on the incremental conductance algorithm was used to improve the PV efficiency. The equation (5) is employed to calculate the result. Fig. 3 shows the PV cell properties at different levels of irradiance and at a steady temperature of 250C. In Fig. 2, the control system is illustrated.

$$P_{PV} = V_{PV}.I_{PV} \quad (5)$$

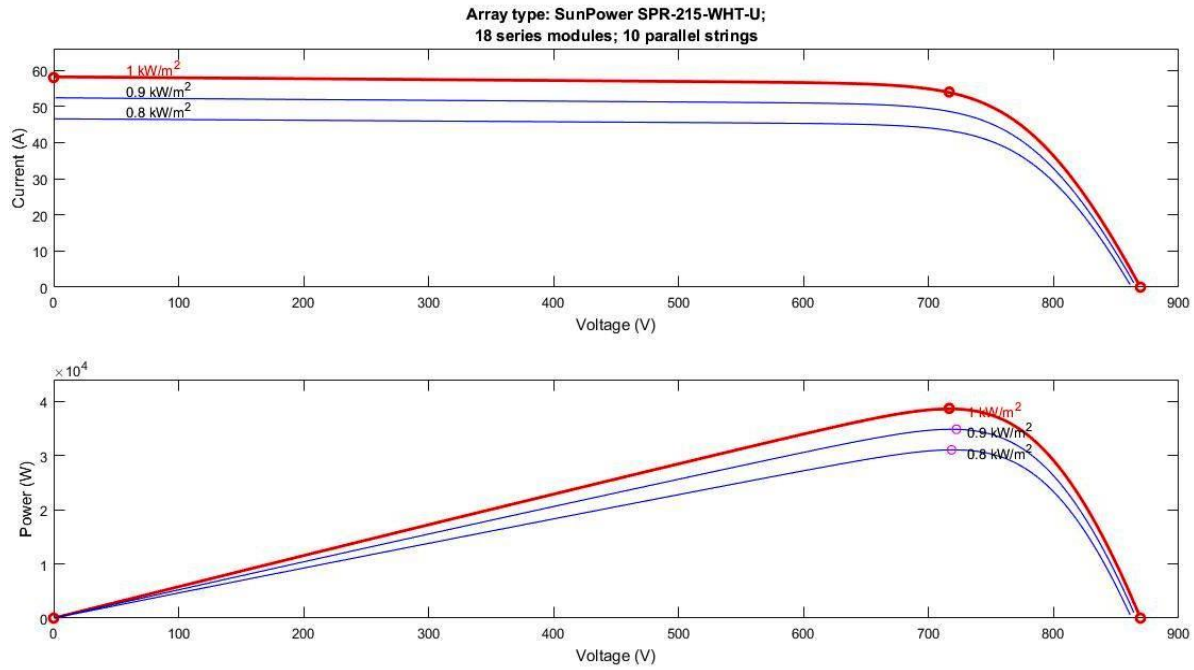

Figure 3: PV cell characteristics at various irradiation and constant temperature 25^0c

International Journal on Recent and Innovation Trends in Computing and Communication
ISSN: 2321-8169 Volume: 11 Issue: 9
Article Received: *25 July 2023* ***Revised:*** *12 September 2023* ***Accepted:*** *30 September 2023*

2.2 Battery system

The quantity of solar power generated (SPG) while meeting SOCB limitations to maintain DC voltage determines the battery's charging and discharging mode of operation, which is determined by Eq. (6) state of charge of battery (SOCB) limits provided by Eq. (7). Table 2 lists the DC link's operational modes. In Fig. 4, the control system is displayed.

$$SOCB = 70(1 + \int i_{BS}\ dtQ) \tag{6}$$

$$SOCB_{\min} \le SOCB \le SOCB_{\max} \tag{7}$$

2.3 Wind system

Once rectified from the AC voltage is produced by the wind power generation (WPG) system. In this work, a permanent magnet synchronous machine was examined. Equations (8) through (12) provide the wind power generation depicted in Fig. 4.

$$P_m = 1/2\pi\ \rho\, C_p(\lambda,\beta)\, R^2\, V^3 \tag{8}$$

$$\lambda = \frac{\omega_m R}{v} \tag{9}$$

$$\omega_m = \omega_t\ G_r \tag{10}$$

$$C_p(\lambda,\beta) = 0.23\left(\frac{116}{\lambda_1} - 0.48\beta - 5\right)\exp^{\frac{-12.5}{\lambda_1}} \tag{11}$$

$$\lambda_1 = \left(\frac{1}{\frac{1}{\lambda - 0.02\beta} - \frac{0.0035}{3\beta + 1}}\right) \tag{12}$$

Table 2: Power at DC link (P_{DC})

Modes of operation (if)	(then) Action
1 . SPG and WPG=0	BES = P_{DC} .
2 . *SPG* & *WPG*= P_{DC}	*SPG* & *WPG*= P_{DC} .
3. *SPG* & *WPG* < P_{DC}	P_{DC}-(SPG+WPG) = Battery will supply until $SOCB_{\min}$.
4 .*SPG* & *WPG* > P_{DC}	(SPG+WPG)- P_{DC} = Battery charges until $SOCB_{\max}$

3. DESIGN OF PARAMETERS

The shunt power filters' primary function is to deliver supply current without distortion by injecting the necessary amount of current at the PCC. The control system uses Equation.13 to determine the required quantity of injection current.

$$i_s = i_l - i_{sh} \tag{13}$$

$$V_s = V_m \sin wt \tag{14}$$

$$i_l = \sum_{n=1}^{\infty} i_n \sin(nwt + \phi_n) = i_1 \sin(wt + \phi_1) + \sum_{n=1}^{\infty} i_n \sin(nwt + \phi_n) \tag{15}$$

$$P_l = V_s * i_l \tag{16}$$

International Journal on Recent and Innovation Trends in Computing and Communication
ISSN: 2321-8169 Volume: 11 Issue: 9
Article Received: *25 July 2023* ***Revised:*** *12 September 2023* ***Accepted:*** *30 September 2023*

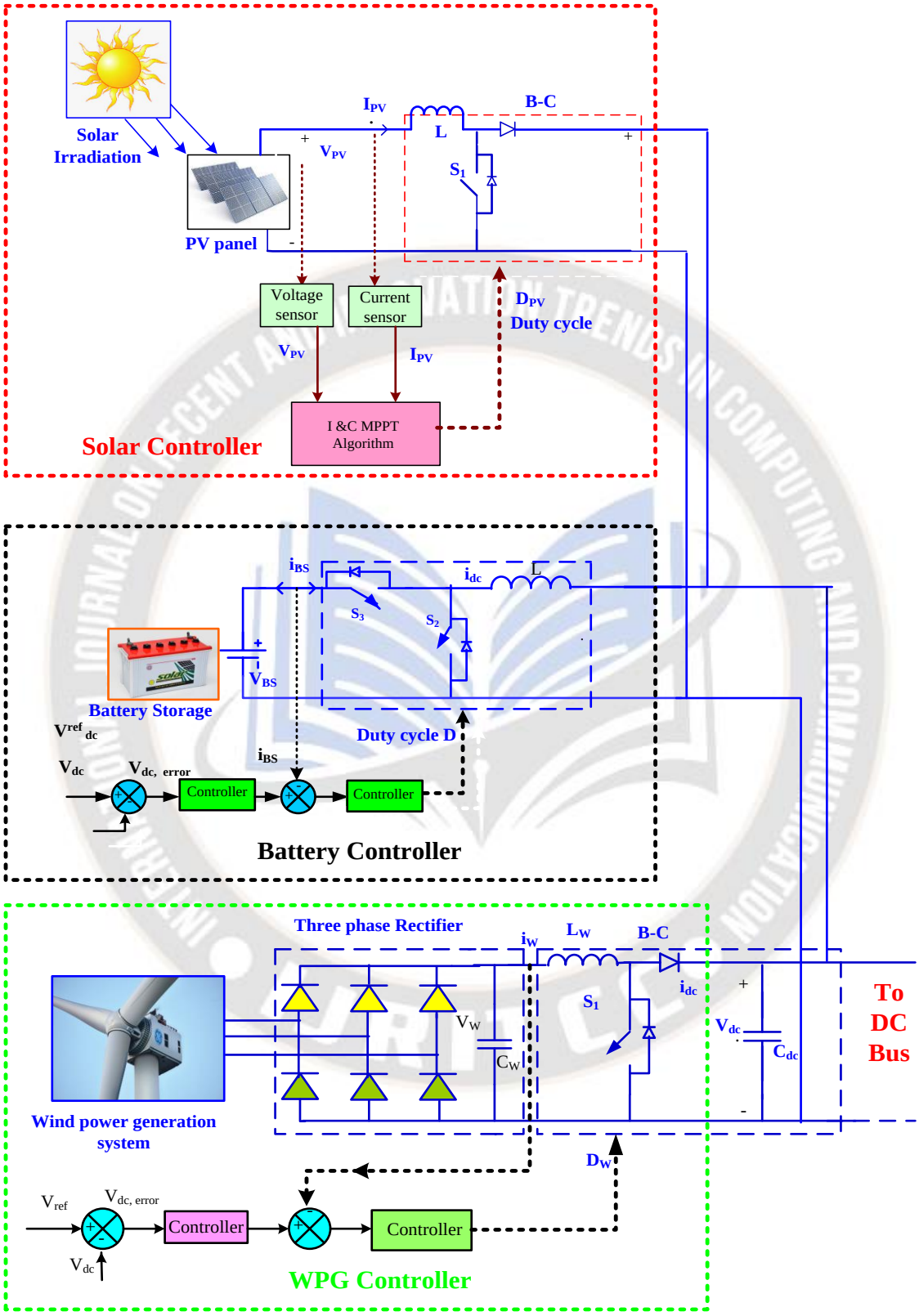

Figure 4: Battery control system with B-B-C

International Journal on Recent and Innovation Trends in Computing and Communication
ISSN: 2321-8169 Volume: 11 Issue: 9
Article Received: *25 July 2023* ***Revised:*** *12 September 2023* ***Accepted:*** *30 September 2023*

4. STF CONTROL

The fluctuating load behavior of the system leads to unexpected emergence of faults causing changes in the DLCV. However to make the DC voltage steady in a short amount of time without overshooting is therefore highly crucial. An ordinary control system typically comprises of a PLL and a STAPF. While the purpose of PLL is to separate the positive sequence from the source voltage, this recommended solution uses STF-based UVGT to separate the current into its FC and HC while also producing PSY from the distorted supply voltage. LPF also performs the function of HPF. Therefore, the single STF, STAPF, is used in the approach proposed in this paper. Given that the STF-UVGM and STF-αβ0-dq0 transformations are accessible in [25] the design part of proposed ANN-SMC was discussed in detail below:

4.1 Shunt VSC

The primary function of STAPF is to lower current signal distortions, which lowers THD by providing the proper compensating current and controlling DLCV. During dynamic load fluctuations, ANN-SMC is used to minimize THD and regulate the steady DLCV in a brief amount of time. The controller for the suggested approach is shown in Figure 5.

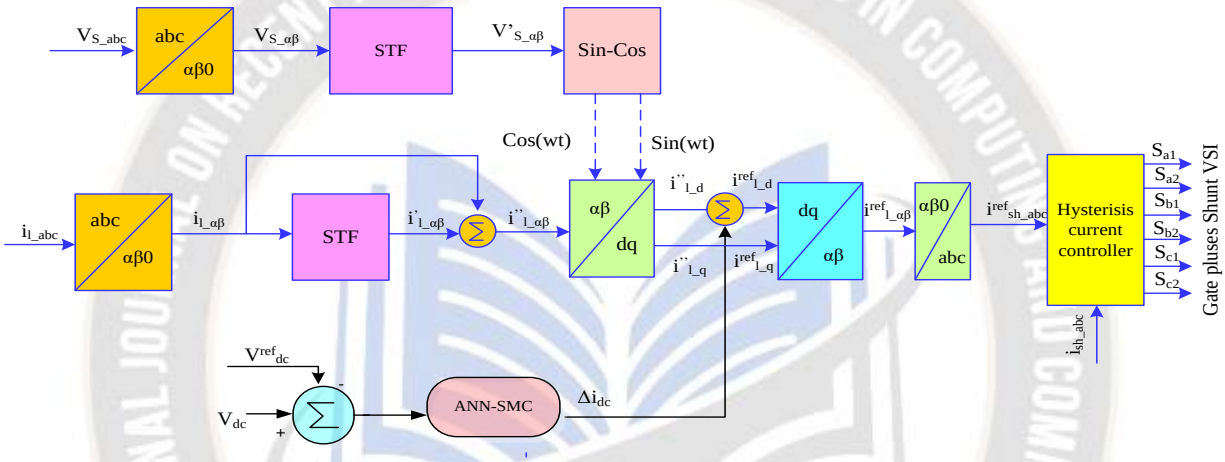

Figure 5: ANN-SMC for Shunt Converter

4.1.1 Proposed ANN-SMC for DLCV balancing

By injecting compensating current, it controls DC link balancing during faults and dynamic loading circumstances. An input layer (IL), a hidden layer (HL), and an output layer (OL) make up the structure of an ANN. The input data is gathered by IL and sent to the HL. It is then multiplied by the corresponding weights on the linked links that connect the IL and HL. In this case, calculations are performed on HL with a chosen bias, and the results are accumulated in OL.

In this work, the controller that uses an ANN based on error back propagation (BP) is chosen. To get the intended result, the weights of the link are adjusted during training by analyzing the error. During ANN training where the performance function is MSE, the LMBP training method is employed. The LMBP algorithm updates the weight using the generated derivatives, which have the advantages of rapid convergence and effective learning [32]. The ANN controller used for this DLCV balance includes one input, one output, and one hidden layer that has 100 neurons Fig. 6.

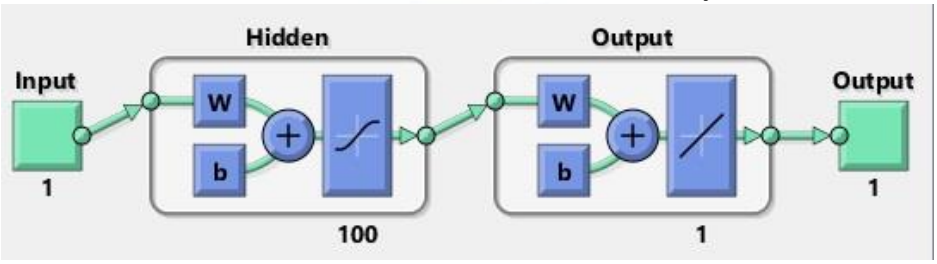

Figure 6: DLCV balancing ANN structure

International Journal on Recent and Innovation Trends in Computing and Communication
ISSN: 2321-8169 Volume: 11 Issue: 9
Article Received: *25 July 2023* ***Revised:*** *12 September 2023* ***Accepted:*** *30 September 2023*

Every single neuron in multilayer perceptron networks has an activation and summation function. However, these neurons among the layers are interconnected with some numerical weights. The summing function's work is to multiply the bias by the sum of the inputs and weights, as shown in Eq. (16). Here, β_k is a bias, the weight w_{pk} connects the p and k neurons. and m is the number of inputs. The sigmoid function, as provided by Eq. (17), is typically utilized as an activation function for nonlinearity. As a result, Eq. (19) shows the output of the k neuron [24].

$$S_k = \sum_{p=1}^{m} w_{p_k} I_p + \beta_k \quad (17)$$

$$f(x) = \frac{1}{1+e^{-x}} \quad (18)$$

$$O_k = f_k\left(\sum_{p=1}^{m} w_{p_k} I_p + \beta_k\right) \quad (19)$$

Here, n is the total instances, $\overline{O}$ the expected, O received outputs and *MSE* is assessed using Eq. (20).

$$MSE = \frac{1}{n}\sum_{p=1}^{m} (O_p - \overline{O}_p)^2 \quad (20)$$

4.1.2 Sliding Mode Controller

A sliding mode controller (SMC) is a type of control system used in engineering and control theory to achieve robust and precise control of dynamic systems. It is particularly effective for controlling systems with uncertainties, disturbances, and nonlinearities. The key concept behind the sliding mode control is to create a sliding surface in the state space of the system and drive the system's state trajectory onto this surface and maintain it there.

The basic idea of a sliding mode controller can be as follows:

- Sliding Surface: A sliding surface is a hyper-plane or a sub manifold in the state space of the system. It is defined depending on the desired behavior of system.
- Control Law: The control law is designed such that it drives the system's state onto the sliding surface and maintains it there. The controller's objective is to keep the system's trajectory sliding along this surface.
- Sliding Mode: When the system's state lies on the sliding surface, it enters a sliding mode. In this mode, the system's dynamics are simplified, making it easier to control.

Here, Eq. (21) is used to evaluate the error.

$$x_1 = V^{ref}{}_{dc} - V_{dc} = err(n) \quad (21)$$

The Eq. (22) provides the derivative of the estimated error.

$$x_2 = \frac{1}{T}e(n) - err(n-1) \quad (22)$$

Here, T is a time period, and x_1 and x_2 are variables in state space whose expression is Eq. (23)

$$\dot{x} = \begin{bmatrix} \dot{x}_1 \\ \dot{x}_2 \end{bmatrix} = \begin{bmatrix} 0 & 1 \\ 0 & 0 \end{bmatrix}\begin{bmatrix} x_1 \\ x_2 \end{bmatrix} + \begin{bmatrix} 0 \\ -k \end{bmatrix}\mu \quad (23)$$

However, Eqs. (24) and (25) each represent the sliding plane's state space equations.

$$s = \begin{bmatrix} C & 1 \end{bmatrix}\begin{bmatrix} x_1 \\ x_2 \end{bmatrix} = Cx_1 + x_2 \quad (24)$$

$$\dot{s} = \begin{bmatrix} C & 1 \end{bmatrix}\begin{bmatrix} \dot{x}_1 \\ \dot{x}_2 \end{bmatrix} = C\dot{x}_1 + \dot{x}_2 \quad (25)$$

According to the power rate law,

$$\dot{s} = -L|s|^{\alpha}\,\mathrm{sgn}(s) \quad (26)$$

Here,

$$\mathrm{sgn}(s) = \begin{Bmatrix} 1 \\ -1 \end{Bmatrix} \; for \; \begin{matrix} s > 0 \\ s < 0 \end{matrix} \quad (27)$$

The Eqs. (28) are used to calculate the μ control law.

$$\mu = \frac{1}{K}\left[Cx_2 + L|s|^{\alpha}\,\mathrm{sgn}(s)\right] \quad (28)$$

The goal of training the ANN-SMC controller is to produce signals of reference current while keeping a constant DLCV. Nevertheless, in order to keep the DLCV steady, the real and reference DLCVs are evaluated, and the difference between them is selected as the input data (Δi_{dc}).

5. RESULTS AND DISCUSSION

The 3ω distribution system was selected to observe the performance of the proposed ANN-SMC. The system was developed in Matlab version 2016 given in Figure 7. Four different test cases with several arrangement of non-liner balanced and unbalanced loads, variable irradiation with constant 25^0c temperature were chosen to analyze the working of ANN-SMC as listed in Table-5. However, the THD were evaluated for all test cases in addition to the comparison with PI-C, SM-C, ANNC methods along with controllers that are present in the survey as listed in Table 6. The selected shunt and load ratings in this work are given in Table 4.

International Journal on Recent and Innovation Trends in Computing and Communication
ISSN: 2321-8169 Volume: 11 Issue: 9
Article Received: *25 July 2023* ***Revised:*** *12 September 2023* ***Accepted:*** *30 September 2023*

Table 4: Shunt converter ratings with loads considered

Supply	L_s = 1e-3 H, V_s = 380V ; f = 50Hz
SUAPF	C_{sh} = 6E-6 F; L_{sh} = 1e-3 H
DClink	C_{dc} : 2200 microfarad ; $V^{ref}{}_{dc}$ = 700Volts

At this point of case-1, as shown in Table 5, Load 2 & 4 was chosen to demonstrate how well STAPF works for balanced loads. As demonstrated in Fig. 8(a), the developed approach reduces current signal imperfections that reflect in the THD. Initially, the grid is supplied till 0.2 sec after that island microgrid supplies to the load. As indicated in Table 6, the supply current signal THD is reduced to 4.27%, which appears to be lower. Furthermore, as shown in Figure 8(b), the controller maintains a steady DLCV at 1000W/m2 irradiation, 11 m/sec, and a constant temperature of 250 c.

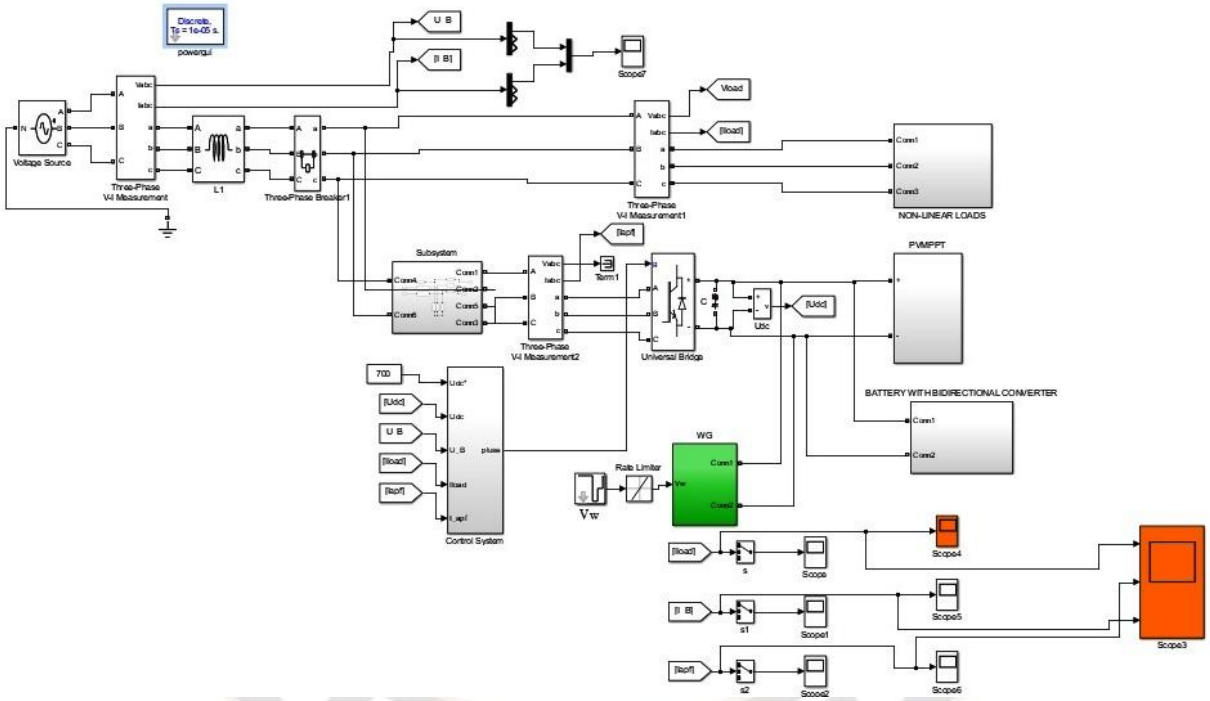

Figure 7: Shunt filter model with loads in Simulink

In case 2, till 0.2sec load 1 is connected at 0.2sec load 3 is connected to an islanded micro-grid with variable irradiation and a wind speed of 11 meters per second. As observed in Figure 9(a) and Figure 9(b), the suggested ANN-SMC successfully suppresses the THD to 3.45% and keeps the DLCV constant under irradiation and load change. However, the suggested technique just lowers the load current's harmonics.

In scenario 3, load 1 is connected for 0.2 seconds, just like in cases 1 and 2. Loads 3 and 4 were connected after 0.2 seconds. As shown in fig. 10(a), the suggested ANFIS lowers harmonics, which reflects THD to 4.45%, below IEEE norms. As seen in Fig. 10(b), it also maintains the DLCV constant under 1000 w/m2 of radiation and fluctuating wind speeds.

In example 4, load 2 and 4 were selected with varying wind speed and irradiation. As seen in Fig. 11(a), the ANFIS reduces the THD to 4.57% and suppresses the distortions in the current signal. On the other hand, Fig. 11(b) demonstrates that the proposed ANFIS operates effectively under load, solar irradiation, and wind velocity all at once. Furthermore, Fig. 12 displays the THD frequency spectrum for each scenario.

International Journal on Recent and Innovation Trends in Computing and Communication
ISSN: 2321-8169 Volume: 11 Issue: 9
Article Received: *25 July 2023* ***Revised:*** *12 September 2023* ***Accepted:*** *30 September 2023*

Table 5: Test cases

Condition / Load	Case1	Case2	Case3	Case-4
Load 1: Rectifier load R=5, L= 30e-3	✓	✓	✓	✓
Load 2 : P= 20e3 Watts, Q= 100vars	✓		✓	✓
Load 3 : R= 15, L= 5e-3H; R= 10, L= 30e-3H; R= 5, L= 15e-3H			✓	
Load 4: Induction motor LC = 400 mH, 50 μF, R = 500 Ω	✓	✓	✓	✓
Constant irradiation of 1000W/m2	✓		✓	
Variable irradiation		✓		✓
Constant wind velocity of 11m/sec	✓	✓		
Variable wind velocity			✓	✓
Current	✓	✓	✓	✓
THD	✓	✓	✓	✓

Table 6 % THD comparison

Method	Case1	Case2	Case3	Case4
PIC	5.82	7.68	5.25	6.01
SMC	4.55	4.74	4.23	5.01
ANNC	4.29	3.45	3.05	4.70
ANN-SMC	**4.27**	**3.45**	**4.45**	**4.70**

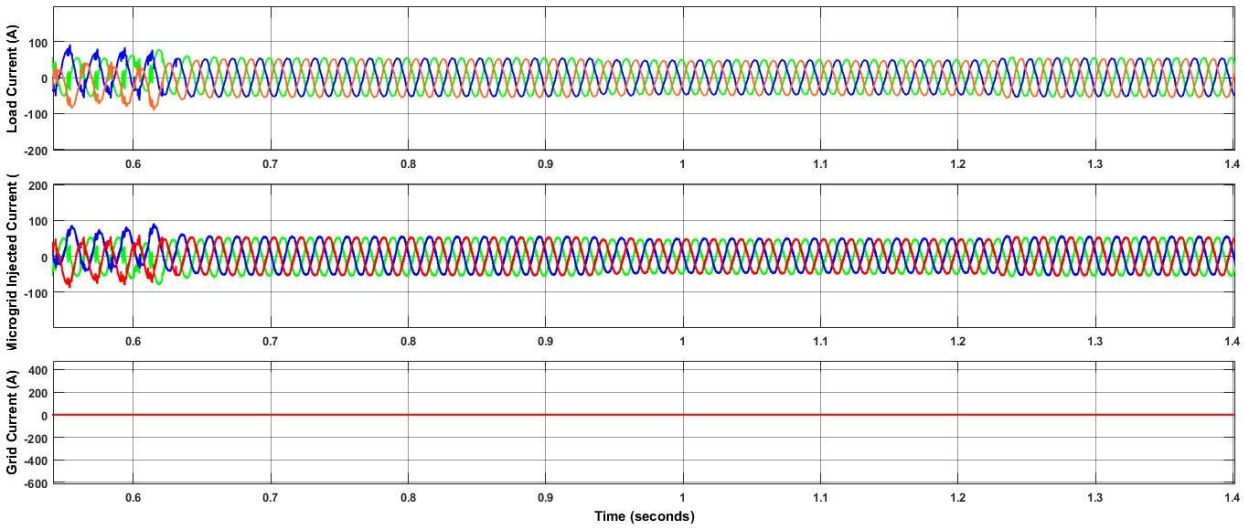

(a) i_l, i_{sh}, i_S

International Journal on Recent and Innovation Trends in Computing and Communication
ISSN: 2321-8169 Volume: 11 Issue: 9
Article Received: *25 July 2023* ***Revised:*** *12 September 2023* ***Accepted:*** *30 September 2023*

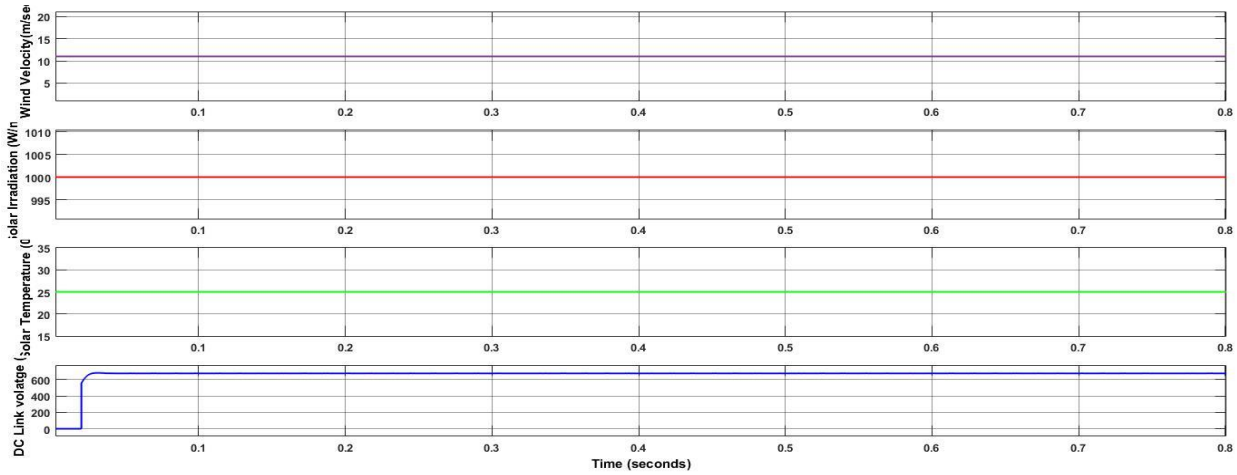

(C) irradiation, T, DLCV

Figure 8: Proposed system for case-1

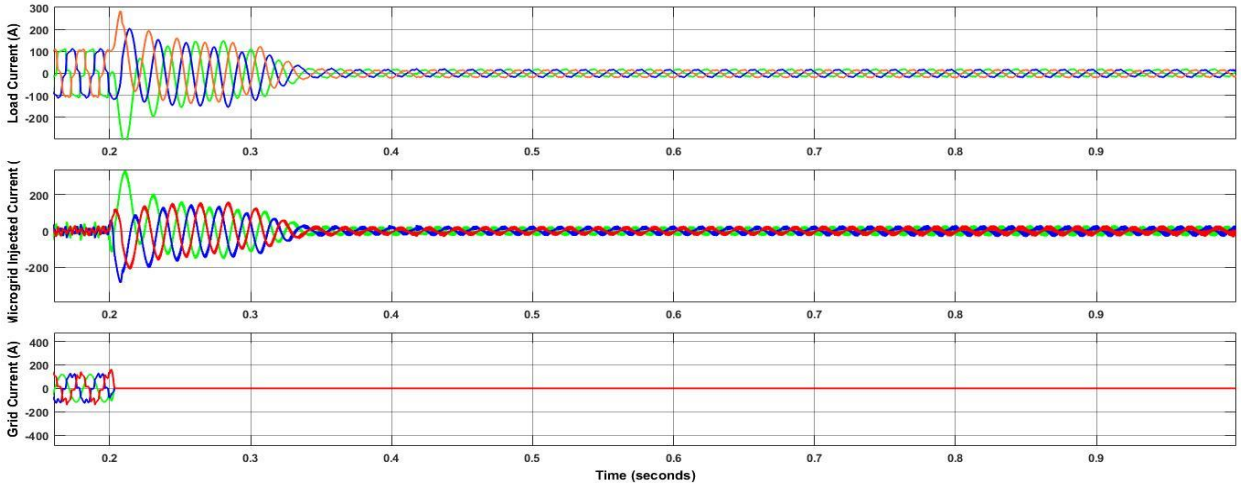

(a) i_l, i_{sh}, i_S

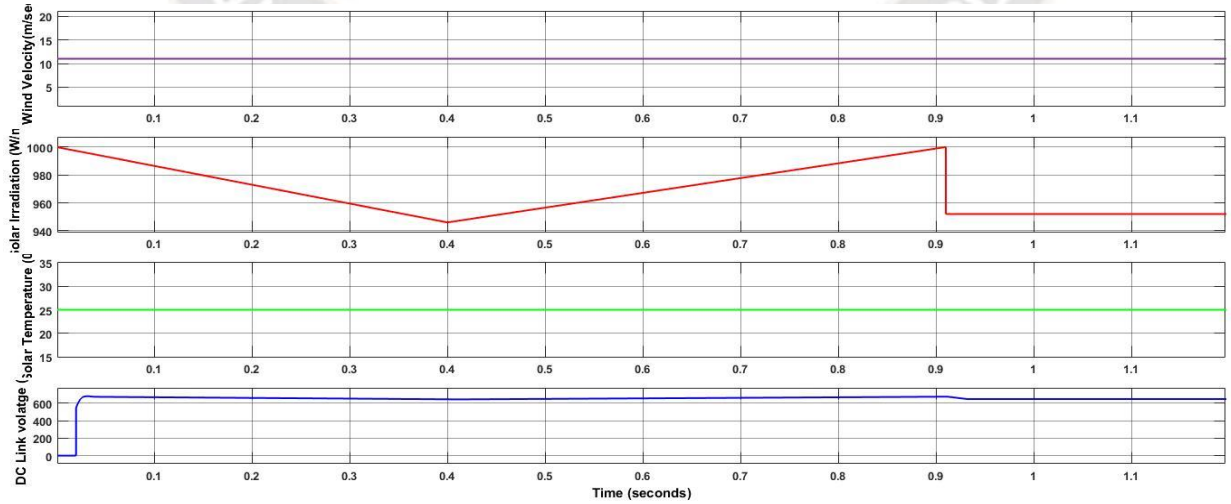

(b) irradiation, T, DLCV

Figure 9: Proposed system for case-2

International Journal on Recent and Innovation Trends in Computing and Communication
ISSN: 2321-8169 Volume: 11 Issue: 9
Article Received: *25 July 2023* ***Revised:*** *12 September 2023* ***Accepted:*** *30 September 2023*

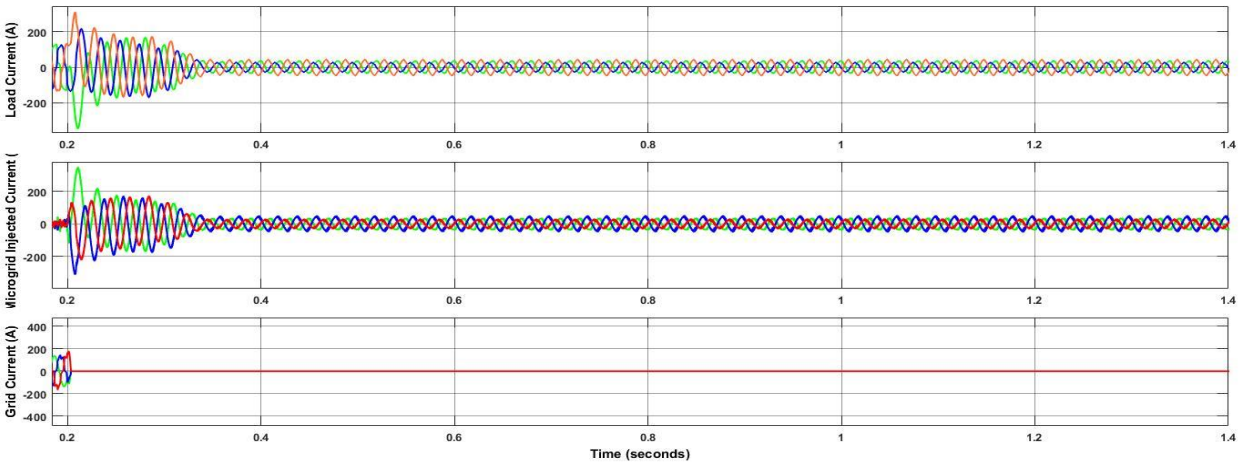

(a) i_l, i_{sh}, i_S

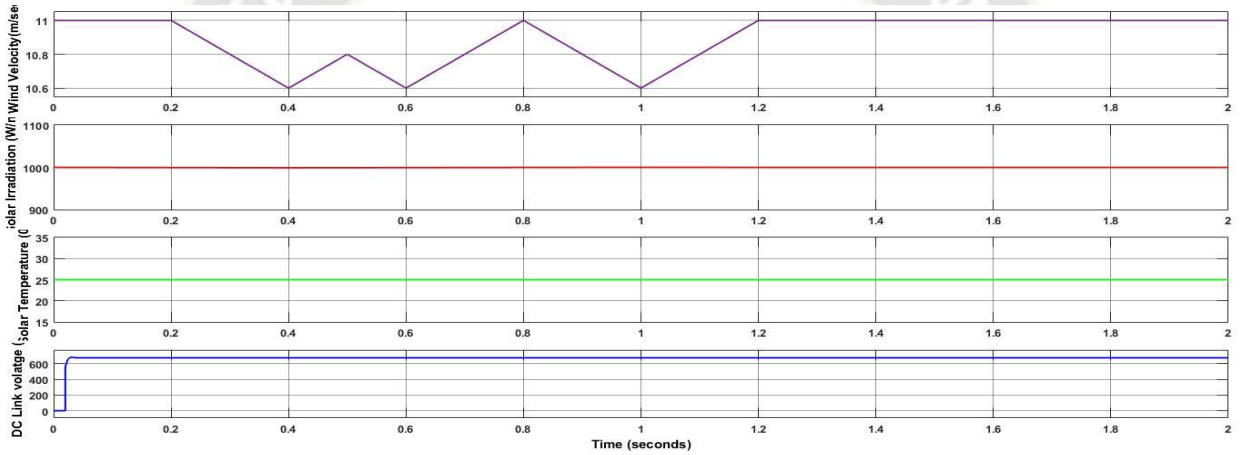

(b) irradiation, T, DLCV

Figure 10: Proposed system for case-3

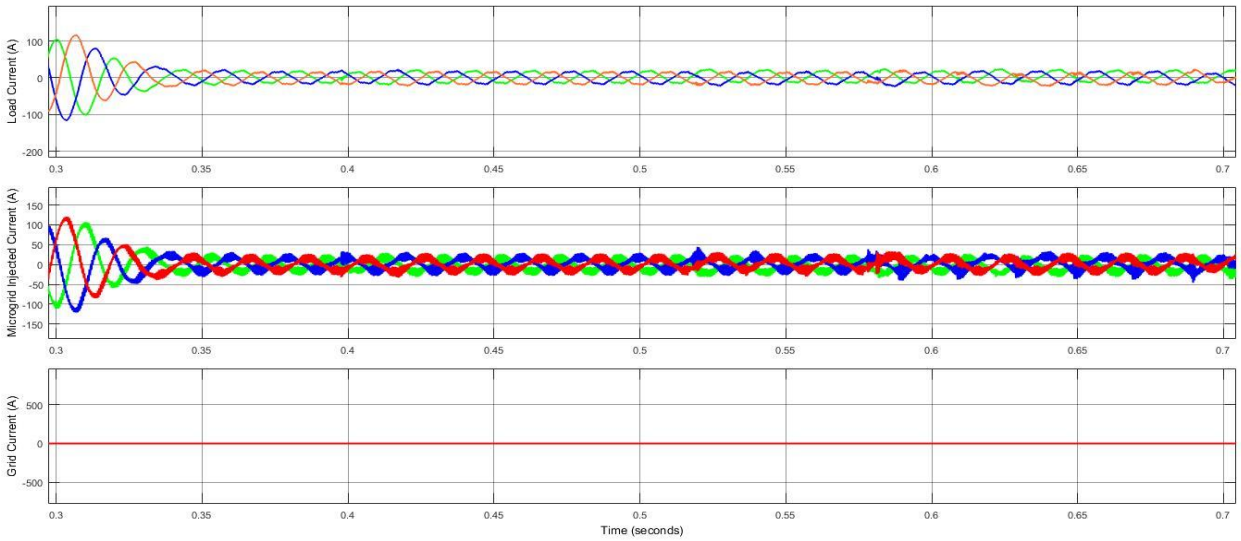

(a) i_l, i_{sh}, i_S

International Journal on Recent and Innovation Trends in Computing and Communication
ISSN: 2321-8169 Volume: 11 Issue: 9
Article Received: *25 July 2023* ***Revised:*** *12 September 2023* ***Accepted:*** *30 September 2023*

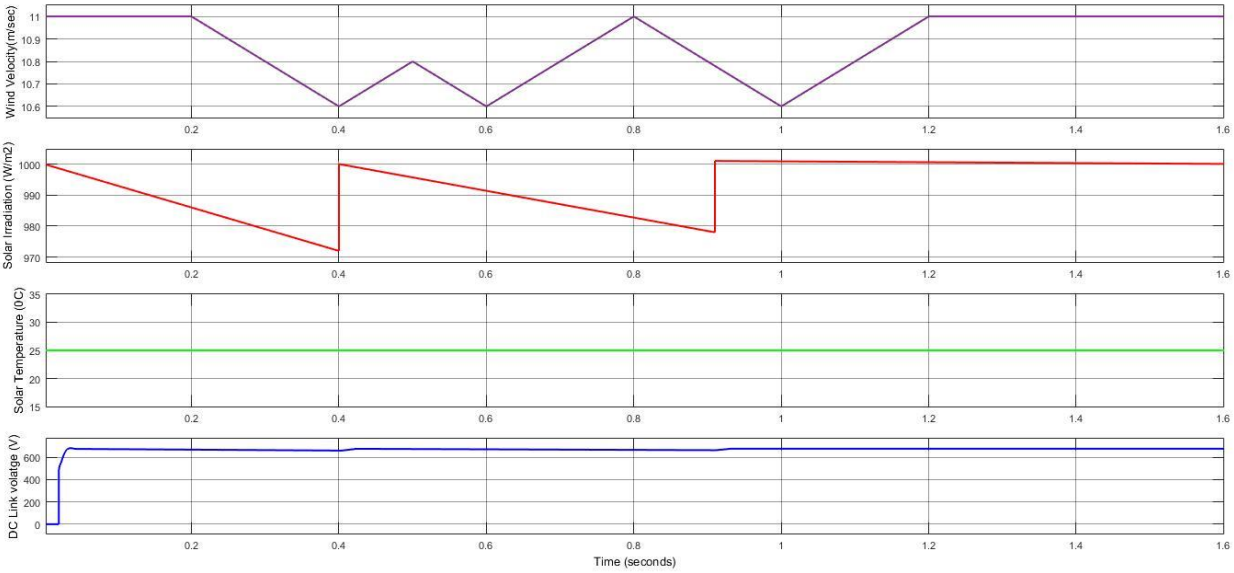

(b) irradiation, T, DLCV

Figure 11: Proposed system for case-4

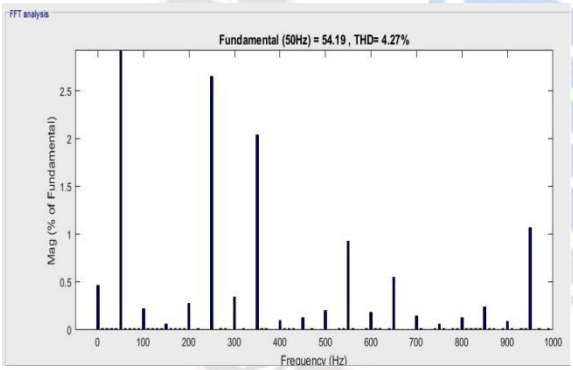

Case-1

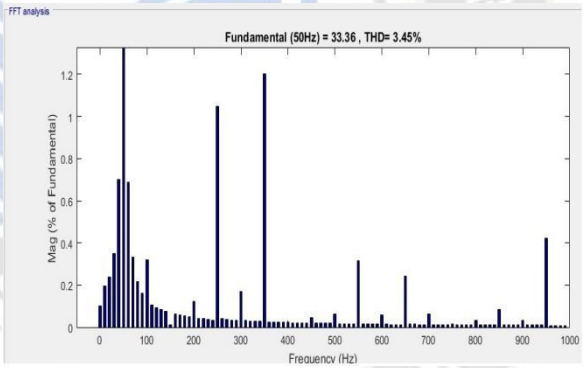

Case-2

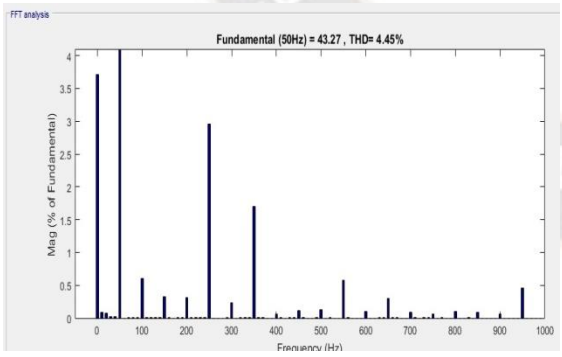

Case-3

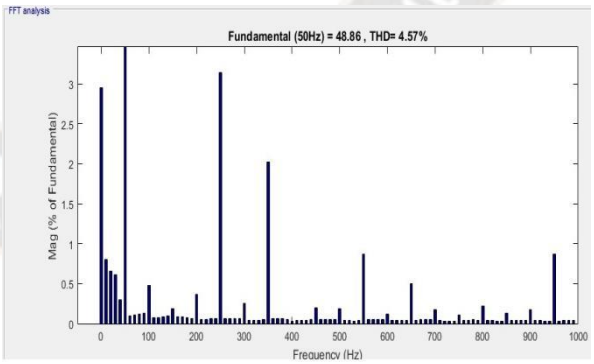

Case-4

Figure 12: THD spectrum

6. CONCLUSION

The ANN-SMC is designed for Solar, wind and BES (microgrid) integrated shunt VSC with an objective of regulating DLCV and reducing THD and to observe the performance of the system under constant solar temperature 25^{o}c during variable load, solar irradiation, and wind velocity.

The STF is developed to eliminate the necessity of PLL. From the observation of the performance of developed technique on four different combinations of test studies it clearly exhibits that it diminishes the load current THDs. Moreover, by the comparative investigation with PI-C, SM-C and ANNC it is has been proved that the performance of developed method was much better than other controllers.

REFERENCE

1. Vijayakumar Gali, Nitin Gupta, R. A. Gupta, "Mitigation of power quality problems using shunt active power filters: A comprehensive review**"** 12th IEEE Conference on Industrial Electronics and Applications (ICIEA)**,** 18-20 June 2017.
2. Metin Kesler and Engin Ozdemir, "Synchronous-Reference-Frame-Based Control Method for UPQC under Unbalanced and Distorted Load Conditions", IEEE Transactions on Industrial Electronics, DOI: 10.1109/TIE.2010.2100330, Vol. 58, No. 9, pp. 3967-3975, September 2011.
3. Suresh M and Panda A. K, "PI and Fuzzy Logic Controller based 3-phase 4-wire Shunt active filter for mitigation of Current harmonics with Id-Iq Control Strategy", Journal of power Electronics , DOI:10.6113/JPE.2011.11.6.914, Vol. 11, No. 6, Nov 2011.
4. Soumya R. Das, Prakash K. Ray, Asit Mohanty; Gayadhar Panda, "Power Quality Enhancement in PV and Battery Storage Based Microgrid Using Hybrid Active Filter" 2020 3rd International Conference on Energy, Power and Environment: Towards Clean Energy Technologies, 5-7 March 2021.
5. Suresh M and Panda A. K, "RTDS hardware implementation and simulation of STAPF for mitigation of harmonics using p-q control strategy with PI and Fuzzy logic controllers", Frontiers of Electrical and Electronic Engineering , DOI:10.1007/s11460-012-0198-7,Vol. 7, No. 4, pp. 427–437, Jun. 2012.
6. Hsiung C L, "Intelligent Neural Network-Based Fast Power System Harmonic Detection," IEEE Transactions on Industrial Electronics, DOI: 10.1109/TIE.2006.888685 , Vol. 54, No. 1, Feb.2007.
7. P.K.Dash S.K.Panda T.H.Lee J.X.Xu, A.Rou tray, "Fuzzy and Neural Controllers for Dynamic Systems: an Overview". IEEE, May 1997.
8. Shravan Kumar Yadav, B. Sabitha & Anush Prabhakaran (2023) O ptimal Placement of UPQC in Distribution Network Using Hybrid Approach, Cybernetics and Systems, 54:7, 1014-1036, DOI: 10.1080/01969722.2022.2129378
9. S.S. Dheeban & N.B. Muthu Selvan (2023) ANFIS-based Power Quality Improvement by Photovoltaic Integrated UPQC at Distribution System, IETE Journal of Research, 69:5, 2353-2371, DOI: 10.1080/03772063.2021.1888325
10. D. Krishna, M. Sasikala & V. Ganesh (2022) Adaptive FLC-based UPQC in distribution power systems for power quality problems, International Journal of Ambient Energy, 43:1, 1719-1729, DOI: 10.1080/01430750.2020.1722232
11. K R Suja & I J Raglend (2013) Adaptive Genetic Algorithm/Neuro-Fuzzy Logic Controller Based Unified Power Quality Conditioner Controller for Compensating Power Quality Problems, Australian Journal of Electrical and Electronics Engineering, 10:3, 351-361, DOI: 10.7158/1448837X.2013.11464384
12. Shashi Gandhar, Jyoti Ohri & Mukhtiar Singh (2022) A mathematical framework of ANFIS tuned UPQC controlled RES based isolated microgrid system, Journal of Interdisciplinary Mathematics, 25:5, 1467-1477, DOI: 10.1080/09720502.2022.2046332
13. Sudheer Vinnakoti & Venkata Reddy Kota (2021) Performance analysis of ANN-based multilevel UPQC under faulty and overloading conditions, International Journal of Ambient Energy, 42:13, 1516-1528, DOI: 10.1080/01430750.2019.1611645
14. Mallikarjuna Golla, S. Sankar, K. Chandrasekaran, Renewable integrated UAPF fed microgrid system for power quality enhancement and effective power flow management, International Journal of Electrical Power & Energy Systems, Volume 133, 2021, 107301, https://doi.org/10.1016/j.ijepes.2021.107301.
15. T. Arulkumar, N. Chandrasekaran, Development of improved sparrow search-based PI controller for power quality enhancement using UPQC integrated with medical devices, Engineering Applications of Artificial Intelligence, Volume 116, 2022, 105444, https://doi.org/10.1016/j.engappai.2022.105444.
16. Mohamed Abdusalama, Philippe Poureb, Shahram Karimia, ShahrokhSaadatea, "New digital reference current generation for shunt active power filter under distorted voltage conditions", Vol. 79, pp. 759–765, Dec 2009.

17. Subanth Williams A., Suja Mani Malar R., Ahilan T., Wind connected distribution system with intelligent controller based compensators for power quality issues mitigation, Electric Power Systems Research, Volume 217, 2023, 109103, https://doi.org/10.1016/j.epsr.2022.109103.
18. N.C. Sai Sarita, S. Suresh Reddy, P. Sujatha, Control strategies for power quality enrichment in Distribution network using UPQC, Materials Today: Proceedings, Volume 80, Part 3, 2023, 19, Pages 2872-2882, https://doi.org/10.1016/j.matpr.2021.07.053.
19. S. Poongothai, S. Srinath, Power quality enhancement in solar power with grid connected system using UPQC, Microprocessors and Microsystems, Volume 79, 2020, 103300, https://doi.org/10.1016/j.micpro.2020.103300.
20. Koganti Srilakshmi, Canavoy Narahari Sujatha, Praveen Kumar Balachandran, Lucian Mihet-Popa, and Naluguru Udaya Kumar, "Optimal Design of an Artificial Intelligence Controller for Solar-Battery Integrated UPQC in Three Phase Distribution Networks", Sustainability, Vol. 14, No. 21, Oct-2022.
21. Koganti Srilakshmi , Nakka Srinivas , Praveen Kumar Balachandran , Jonnala Ganesh Prasad Reddy, Sravanthy Gaddameedhi, Nagaraju Valluri, Shitharth Selvarajan, Design of Soccer League Optimization Based Hybrid Controller for Solar-Battery Integrated UPQC, IEEE Access, Vol. 10, pp. 107116-107136, 2022, DOI: 10.1109/ACCESS.2022.3211504.